Available online at www.sciencedirect.com
SCIENCE DIRECT®
Journal of Nuclear Materials 351 (2006) 39–46
journal of nuclear materials
www.elsevier.com/locate/jnucmat

Effect of displacement cascade structure and defect mobility on the growth of point defect clusters under irradiation

C.S. Becquart [a,*], A. Souidi [b,c], C. Domain [d], M. Hou [b], L. Malerba [e], R.E. Stoller [f]

[a] Laboratoire de Métallurgie Physique et Génie des Matériaux, Université des Sciences et Technologies de Lille, Université Lille-1, UMR 8517, Bat. C6, F-59655 Villeneuve d'Ascq cédex, France
[b] Physique des Solides Irradiés et des Nanostructures, CP234, Université Libre de Bruxelles, Bd du Triomphe, B-1050 Brussels, Belgium
[c] Centre Universitaire de Saida, BP138, En-nasr, Saida 20000, Algeria
[d] EDF-R&D Département MMC, Les Renardières, F-77818 Moret sur Loing cédex, France
[e] SCKCEN, Reactor Materials Research Unit, B-2400 Mol, Belgium
[f] Metals and Ceramics Division, Oak Ridge National Laboratory, Oak Ridge, TN 37831, USA

Abstract

The existence of an interplay between the structure of displacement cascades and point defect mobility that influences the long-term evolution of primary damage in α-Fe is revealed by applying an object kinetic Monte Carlo (OKMC) method. The investigation was carried out using different parameter sets, which primarily differ in the description of self-interstitial atom (SIA) cluster mobility. Two sets of molecular dynamics cascades (produced with the DYMOKA and the MOLDY codes, using different interatomic potentials) and one set of cascades produced in the binary collision approximation with the MARLOWE code, using a Ziegler–Biersack–Littmark (ZBL) potential were separately used as input for radiation damage simulation. The point defect cluster populations obtained after reaching 0.1 dpa were analyzed in each case and compared. It turns out that the relative influence of using different input cascade datasets on the damage features that evolve depends on which OKMC parameter set is employed.
Published by Elsevier B.V.

1. Introduction

The importance of the detailed features of the primary damage state on the long-term evolution of radiation damage has been often explicitly or implicitly suggested, but not often studied in a systematic fashion. The object kinetic Monte Carlo (OKMC) approach [1] is particularly suitable for this type of study because of its inherent capability to account for the effect of spatial correlations, anisotropy and inhomogeneity in the defect distributions on their mutual interaction and overall evolution. In the past, this approach permitted a demonstration of the importance of the main features of the primary damage state in explaining the different response of Cu and Fe to irradiation [2]. More recently, this approach has been used to try to determine which features of the defect distribution in cascade debris most influence the results of single-cascade annealing and cascade damage accumulation [3,4] in α-Fe. The latter work involved only a relatively simple

* Corresponding author. Tel.: +33 320 436927; fax: +33 320 434040.
E-mail address: charlotte.becquart@univ-lille1.fr (C.S. Becquart).

0022-3115/$ - see front matter Published by Elsevier B.V.
doi:10.1016/j.jnucmat.2006.02.022

and not completely realistic OKMC parameter set and started with both a molecular dynamics (MD) cascade database and a binary collision approximation (BCA) cascade database, as well as with random clouds of point-defects. Here, that previous investigation is extended by considering the effect of using both different OKMC parameter sets and different MD cascade databases, in addition to the BCA database. It turns out that the magnitude of the influence of the primary damage state on the accumulation of cascade damage depends on the OKMC parameter set employed. In particular, this paper discusses the effect of changing the mobility of self-interstitial atom (SIA) clusters in the OKMC simulations.

2. Cascade generation models and analysis methods

Three groups of displacement cascades were used as input for the OKMC simulations. Two were obtained by MD with the MOLDY [5] and DYMOKA [6] codes and one in the BCA with the MARLOWE code [7]. For cascade simulation with DYMOKA, periodic boundary conditions were imposed on a constant volume ensemble of atoms. The embedded-atom-method (EAM) potential developed in [8] for α-Fe was used. At the beginning of the simulation, the system of particles was equilibrated for 5 ps at 600 K, a temperature representative of reactor pressure vessel operating conditions. When the lattice was at thermal equilibrium, one atom, the primary knock-on atom (PKA) was given a momentum corresponding to an energy between 1 and 20 keV. The timestep in the simulation was manually adapted to the PKA velocity, and it could be as low as 10^{-17} s. Once the cascade energy had been mostly dissipated in elastic collisions, a much longer timestep was allowed, i.e. 10^{-16}–10^{-15} s. More details on the procedure can be found in [6]. The method used with the MOLDY code was similar. However, the iron cascade simulations were carried out using a modified version of the Finnis–Sinclair potential [9,10] and the range of cascade energies reached 100 keV. Periodic boundary conditions were imposed on a constant pressure ensemble of atoms, with simulation cells containing up to 5 million atoms for the highest energy simulations. Additional information on this α-Fe cascade database can be found in [11,12]. For details about differences between the potentials used for MD cascade simulations, see also [13].

The MARLOWE package (version 15) offers a variety of displacement models. Collision cascades are modeled as sequences of binary encounters between which atoms move freely along their scattering asymptotes. A potential function is used to estimate the scattering angle and the integral time for each binary collision. The scattered and recoil atomic momenta, as well as the exit asymptote positions, are calculated using a quadrature integration scheme. In the present work, the pair potential suggested in [14] is used in order to match the short range repulsive component of the potential functions used in MD with MOLDY. The binary collisions are chronologically ordered so that time represents the driving parameter in the cascade development. The number of collisions undergone by the moving atoms is limited by a maximum impact parameter value a little smaller than the first neighbor distance. The binding energy of the atoms to their lattice sites is considered constant and direction independent. It is fitted to the cohesive energy in the matrix, as suggested by previous comparison between MD and its BCA [15]. The binding energy in replacement sequences is taken as 0.2 eV, independent of the sequence direction.

In both the MD and BCA models, the contribution of energy loss to electronic excitation is neglected in the trajectory calculations. As a result, all of the cascade energy is dissipated in elastic collisions and is roughly analogous to the damage energy in the well-known NRT model [11]. This is strictly less than what is conventionally called the PKA energy. For example, a cascade (or damage) energy of 50 keV in iron corresponds to a 79 keV PKA energy.

For the sake of clarity, we shall refer to the MD cascades obtained with the Finnis–Sinclair potential and the MOLDY code as MOLDY, DYMOKA refers to the cascades obtained with the Ludwig–Farkas potential and the DYMOKA code, and BCA refers to the cascades obtained with Marlowe and the Ziegler–Biersack–Littmark (ZBL) potential. The vacancy–interstitial recombination radius in MARLOWE was adjusted so that the number of Frenkel pairs obtained in the BCA was the same as that with MOLDY and the Finnis–Sinclair potential.

2.1. Primary damage characterization

2.1.1. Overall cascade structure

Component analysis permits an ellipsoid to be associated to each individual displacement cascade, accounting for its spatial extension and its morpho-

logy on the basis of its intrinsic characteristics [16]. It is thus useful for comparing cascades. The information provided by this method is the direction of three orthogonal axes that are associated to the spatial point defect distribution and the variance of this distribution projected onto them. The major axis has the direction maximizing the variance, α^2, the second maximizes the variance β^2 of the distribution projected onto a plane perpendicular to the first and the third one has the direction minimizing this variance, γ^2. These directions are parallel to the directions of the eigenvectors of the covariance matrix of the point defect distributions and the associated eigenvalues are the variances of the distribution projected onto the directions of the eigenvectors. The problem is hence reduced to the diagonalization of a 3×3 symmetrical real and positive matrix, which is a straightforward operation.

The eigenvectors and eigenvalues naturally define an ellipsoid associated with each cloud of point defects with axes lengths given by the standard deviation of the distributions projected in the directions of the eigenvectors. These ellipsoids define the cascade cores. In what follows, each core volume will be considered as representative of one displacement cascade.

2.2. Internal cascade structure

Point defect distributions within cascades have been characterized in terms of integral pair correlation functions, providing the probability that two point defects are found at a distance less than or equal to the corresponding distance on the abscissa. The pair correlation function used here is defined by

$$g(r) = \frac{1}{N(N-1)} \sum_{i=1}^{N-1} \sum_{j>i}^{N} \delta(r - r_{ij}), \qquad (1)$$

where N is the total number of point defects considered in the whole simulation box and r_{ij} their separation distance. Standard definitions are used to characterize the distributions of vacancies, of interstitials and closest vacancy–interstitial pairs.

In order to determine the defect cluster distribution, the following criterion has been adopted: a point defect (a vacancy or a SIA) belongs to a cluster if there is at least one defect of this cluster situated at a critical distance from this defect. This distance can be decided at will among first nearest neighbor, second nearest neighbor, etc. The size of a cluster of given type equals the absolute value of the difference between the number of interstitials and vacancies associated with it. This cluster analysis procedure is independent of the cluster shape, type and criterion adopted to define and visualize point defects. For instance, independent of whether an interstitial is represented as a single atom or as a dumbbell with two atoms plus the vacant lattice site in the middle (a vacancy–interstitial complex), the procedure leads to the same cluster size. The procedure is however dependent on the critical distance chosen and may miss atoms that belong to the cluster if they are located further away than the chosen cut-off distance.

3. Object kinetic Monte Carlo

The long-term evolution of point defect clusters in α-Fe is modeled by OKMC with the LAKIMOCA code. The OKMC method treats defects as objects with specific positions in a simulation volume. Probabilities for physical transition mechanisms are calculated based on Boltzmann factor frequencies. After a certain event is chosen, time is increased according to a residence time algorithm [17]. The basic aspects of the parameterization used in our code are described in [1]. Three parameter sets were used.

In set I, all SIA clusters (size $m \geqslant 2$) migrate in 1D, with a migration energy $E_m = 0.04$ eV (as in [1]) and a prefactor decreasing with size according to the law: $\nu_0 \cdot m^{-s}$ ($\nu_0 = 6 \times 10^{12}\ s^{-1}$, $s = 0.51$, following Osetsky et al. [18]). Thus, set I embodies the picture of SIA cluster migration that was till recently widely accepted based on MD results. In set II, small clusters ($m < 5$) migrate in 3D with $E_m = 0.4$ eV, as broadly suggested by recent ab initio calculations [19], while larger clusters maintain 1D motion with $E_m = 0.04$ eV. For large clusters the prefactor decreases with $s = 0.51$ and for small ones it decreases with $s = 10$. Finally, set III treats small clusters ($m < 5$) in the same way as set II, but assumes that larger clusters are completely immobile (see Table 1). For vacancy clusters, the same mobility has been used for all three sets: a migration energy of 0.65 eV and a prefactor decreasing with size according to the law $\nu_0 p^{-(m-2)}$ for $m \geqslant 2$ with $p = 100$ and $\nu_0 = 6 \times 10^{12}$ (as in [1]). These sets are summarized in Table 1.

Damage rates of 10^{-6} and 10^{-4} dpa/s were simulated in the OKMC by injecting displacement cascades selected at random from the chosen cascade group until 0.1 dpa was reached. The lower damage

Table 1
Summary of parameter sets for the description of SIA cluster mobility

SIA cluster size	Set I			Set II			Set III		
(E_m in eV)	s	E_m	D	s	E_m	D	s	E_m	D
$m = 1$	–	0.3	3D	–	0.3	3D	–	0.3	3D
$2 < m < 5$	0.51	0.04	1D	10	0.4	3D	10	0.4	3D
$m \geqslant 5$	0.51	0.04	1D	0.51	0.04	1D	Immobile		

rate is typical of high-flux reactor operating conditions, and the higher rate is similar to that obtained during heavy ion irradiation. The cascade energies considered range from 5 to 100 keV, which realistically represents the effect of a reactor PKA spectrum. The simulations were performed in a $200a_0 \times 200a_0 \times 200a_0$ volume, using periodic boundary conditions and a grain size of approximately 2 μm. The irradiation temperature was 70 °C. With all sets, 100 ppm traps for SIA clusters (binding energy 0.65 eV, capture radius 5 Å) were included. This was necessary because of the generally high mobility (sets I and II) of SIA clusters; they can only accumulate in the material if traps exist. These traps are generally associated with C or N atoms, which are known to affect point defect motion due to their binding energy with SIA or vacancies. However in the present model, C and N atoms do not appear explicitly; rather, *generic*, immobile traps that act on SIA are included. The choice of their density, binding energy and capture radius was made so as to reproduce the density of vacancy clusters (of any size) at different doses after neutron irradiation in the experiment of Eldrup and co-workers [20], as reported in [1], where sensitivity studies on the choice of binding energy and capture radius were performed.

4. Primary damage

As shown in previous work [21] the number of Frenkel pairs predicted by the BCA reasonably matches the MD prediction, provided that an interstitial–vacancy recombination radius is adopted and fitted to MD results. When applied to the BCA nascent cascades, the recombination radius affects the number of Frenkel pairs, but not its functional dependence on cascade energy. Thus, the slope is unchanged in a log–log plot of defect production vs. energy. The match between MD and BCA cascades, as well as between independent MD calculations can be observed in the results for iron cascades

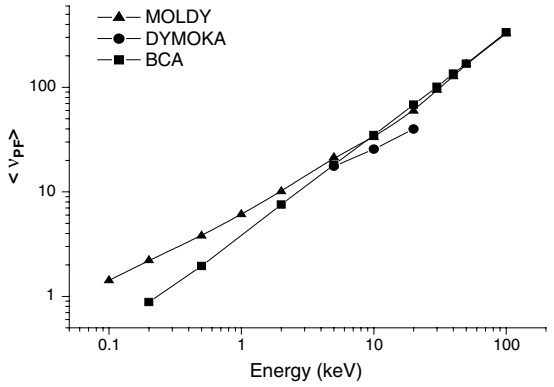

Fig. 1. Mean number of Frenkel pairs obtained by molecular dynamics with the DYMOKA and the MOLDY codes using different potentials. Results obtained in the BCA with the Marlowe code and a ZBL potential are shown as well. They were fitted to MOLDY results for a 50 keV cascade energy by means of a recombination radius of 3.5 lattice units.

shown in Fig. 1. The slope in the MD and BCA energy dependence tend to the same value (close to unity) at high energy, where the ballistic character of collision cascades is expected to dominate. The change in slope for low energy MD cascades relates to the way the cascades develop and thus to the subsequent spatial distribution of the final remaining point defects. The spatial extent of the defect distributions in displacement cascades, characterized by their associated ellipsoid volumes and elongations, is quite broad. These properties were already discussed in [21] for α-Fe. Here, we shall limit ourselves to show the cascade energy dependence on the mean of the distribution of the anisotropy factor, α/γ-1, as defined in [21], shown in Fig. 2. MOLDY, DYMOKA and BCA results agree

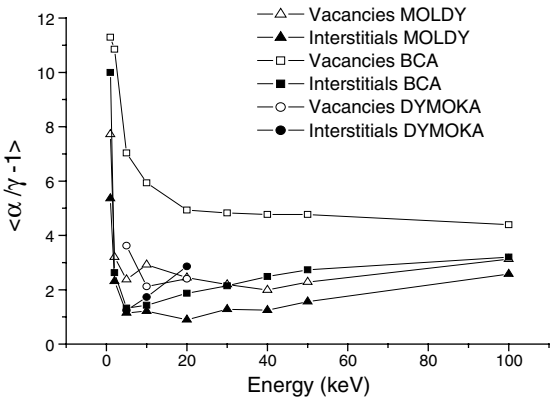

Fig. 2. Anisotropy factor as a function of the cascade energy as obtained for vacancy and interstitial distributions in MOLDY, DYMOKA and MARLOWE cascades.

rather well except for the vacancy distributions obtained in the BCA, that are systematically more anisotropic than predicted by MD. This is no surprise, since vacancies are distributed in the cascade core which, in MD, is affected by a thermal spike at the end of the ballistic phase during which the core/matrix interface is minimized, lowering in this way its excess energy. As far as interstitial distributions are concerned, the anisotropy appears to have a minimum in the 10 keV range. This suggests the occurrence of two regimes. At low energy, cascades have progressively decreasing 2D character. This 2D character was already shown in [22] for cascade energies up to a few keV. In the intermediate energy region, cascades appear to be fully 3D. However, when the cascade energy is increased above a minimum anisotropy value, their development tends to follow a track determined by either the PKA direction or the directions of a few particularly energetic secondary recoils. Therefore, a 1D character of the cascades appears, which becomes increasingly pronounced with increasing cascade energy. Subcascades may form along such tracks, forming spatially correlated small displacement clusters.

The overall morphology of cascades is one of their characteristics. Another, which is anticipated to have an important impact on the long-term evolution of cascades, is the distribution of point defect clusters resulting from their development. Clustering considerably affects defect mobility and hence the kinetics of their further growth and removal at sinks. A result that has already been pointed out in [11,23] is that, at least with the potential used in MOLDY, the fraction of point defects in clusters is not much dependent on the cascade energy above about 5 keV in α-Fe. This is shown in Fig. 3, where the two sets of MD and the BCA cascade results are compared. Although DYMOKA cascades are not available on a large enough energy range to be conclusive on this point, they are in reasonable quantitative agreement with the MOLDY set and the invariance of the fraction in clusters is confirmed, after analysis with the procedure described above. However, our comparisons between different potentials [13] show that by no means do all potentials predict the same invariance. This invariance is found also in the BCA, but the fraction of interstitials in clusters is largely underestimated (by one order of magnitude), while the fraction of vacancies in clusters is overestimated (by a factor 2.5). The physical origin of this difference was already discussed in [21]. Because of their high mobility, this

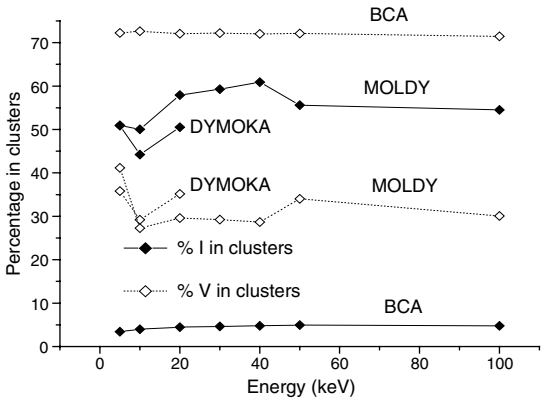

Fig. 3. Percentage of vacancies and interstitials in clusters in cascades obtained by MD with the DYMOKA and MOLDY codes, and by the MARLOWE code in the BCA.

difference in the interstitial clustered fraction may be particularly important in the long-term evolution of BCA and MD cascades. This question is addressed in the next section. Cluster size distributions are seen to differ from one model to another; even the two sets of MD results give different results. On the other hand, this is not surprising, as it has been shown that different potentials do predict different defect clustered fractions [13].

Fig. 4 compares the short distance part of the integrated SIA–SIA pair correlation functions obtained for 20 keV cascades from the two MD sets. BCA results are also shown. As observed earlier [4], the BCA underestimates the number of interstitials having short distance separation. This phenomenon was termed 'aggregation' in order to differentiate it from the first, second or third neighbor distance

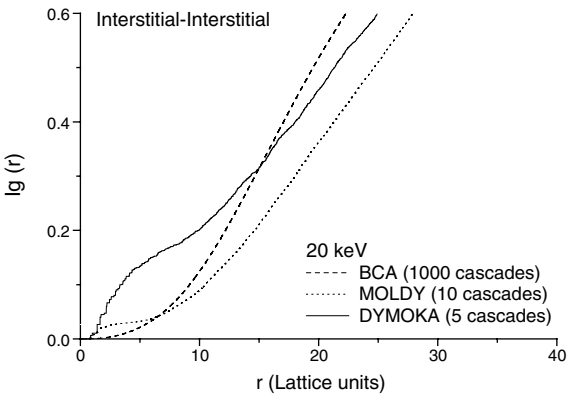

Fig. 4. Integrated interstitial–interstitial radial pair correlation functions obtained for 20 keV cascades generated with the two MD codes and the BCA.

clustering discussed above. This result was initially obtained when comparing BCA with DYMOKA, and is confirmed here for MOLDY as well. Interstitials that are closer together at the end of the cascade may have a larger probability of clustering over longer times, so this difference in the radial pair correlation functions should ultimately lead to different clustering behavior.

5. Long-term evolution

Damage accumulation up to 0.1 dpa was studied using the parameter sets described in Section 2 for damage rates of 10^{-6} and 10^{-4} dpa/s. The microstructural evolution predicted for damage rates differing by two orders of magnitude is found to be rather similar. The results obtained with a damage rate of 10^{-6} dpa/s and with different mobility parameters are shown for comparison in Figs. 5–7. They represent the number density distributions of interstitial and vacancy clusters obtained with the three sets of parameters given in Table 1. In these figures the cluster size is the number of SIA or vacancies. For clarity of the figures, only one set of MD results, those obtained with MOLDY are shown in Figs. 5 and 7. A comparison with DYMOKA is shown only in Fig. 6, but the results with 50 keV and 100 keV cascades as input are not shown. As can be seen in the latter figure, differences exist between the three sets of cascades, but they are smaller than those due to the choice of the parameter set, as discussed in what follows. Let us recall that in Fig. 5 (set I of Table 1), all SIA clusters are highly mobile in 1D. In Fig. 6, all SIA clusters

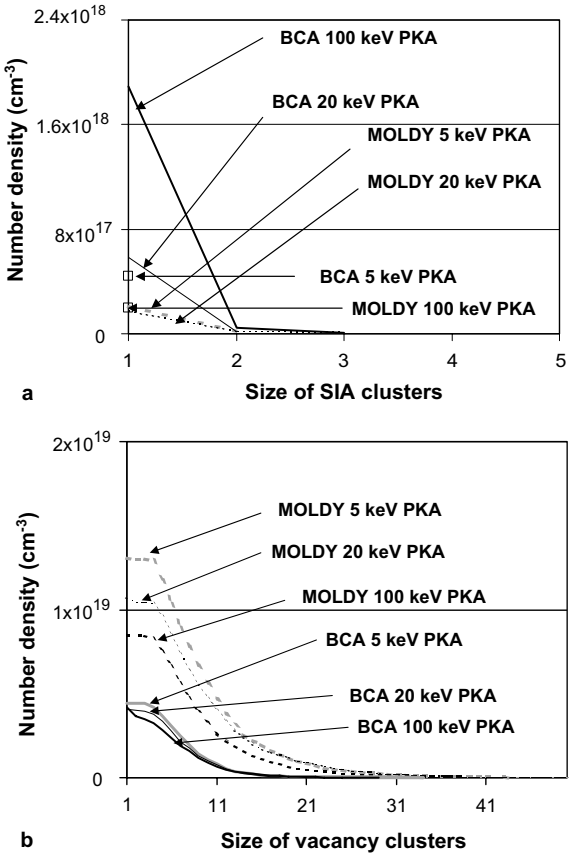

Fig. 5. Cluster number density as a function of cluster size obtained by OKMC with parameter set I. (a) Interstitial clusters and (b) vacancy clusters. Results are given for MOLDY cascades at 100 keV (thick dashed black line), 20 keV (thin dashed black) and 5 keV (thick dashed grey), as well as with MARLOWE BCA cascades at 100 keV (thick solid line), 20 keV (thin solid line) and 5 keV (thick solid grey).

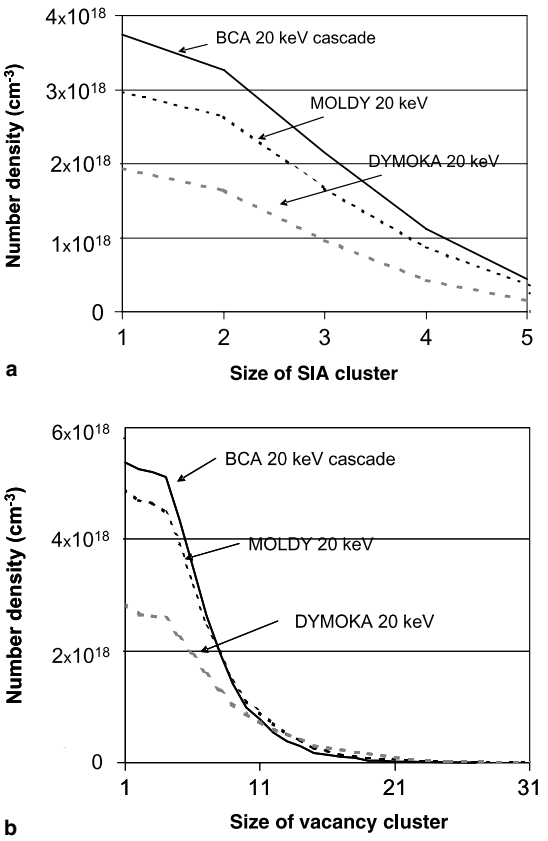

Fig. 6. Same as Fig. 5 with parameter set II. Results are given for 20 keV cascades generated with MOLDY and the Finnis–Sinclair potential (dashed black line), with DYMOKA and the Ludwig–Farkas potential (dashed grey line) and with MARLOWE in the BCA with the ZBL potential (solid black).

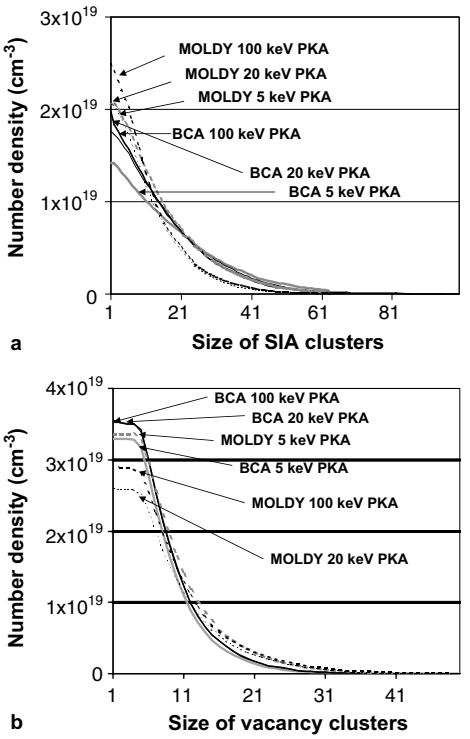

Fig. 7. Same as Fig. 5, but with parameter set III.

are mobile but only the largest ones exhibit the high 1D mobility (set II of Table 1), and in Fig. 7 the largest SIA clusters (larger than 5) are immobile and the smaller ones migrate in 3D as slowly as in Fig. 6 (set III of Table 1).

The results for point defect clusters with these sets of OKMC parameters display two important features:

i. The cluster size distributions obtained by MD and in the BCA are generally similar, with number densities that do not differ by more than about 50% at 0.1 dpa;
ii. Cluster number densities are one to two orders of magnitude higher when large clusters are treated as immobile than when they are treated as mobile (this can be seen by comparing the number densities in Fig. 7 with those in Figs. 5 and 6).

The first feature suggests that for the conditions simulated in the OKMC, the internal structure of the cascades and their spatial extent have only a limited influence on the point defect cluster distributions. The difference found in [4] between BCA and MD for vacancy clusters was larger. For the MD cascades in that study, the density of small vacancy clusters was predicted to be a factor of 2 higher than with BCA and they were still predicted to be a factor of 2 higher than when the initial vacancy positions were chosen at random within similar volumes. However, only single-vacancies and single-SIAs were treated as mobile in those OKMC simulations. By comparing the results in Figs. 5 and 7 to Fig. 6, BCA and MD results differ most when the SIA cluster mobility is the highest or the smallest. Hence, the influence of the internal structure on long-term evolution depends on how the mobility is modeled in the OKMC.

The second feature demonstrates the significance of the mobility of large clusters. The comparison between Figs. 5–7 indicates that the difference in cluster distributions induced by considering big clusters as mobile or not changes the frequencies by more than one order of magnitude. In contrast, using different initial MD or BCA defect configurations induces differences of no more than about 50% in the long-term evolution, with all the mobility models considered. Thus, in this respect, the results do not appear to be highly sensitive to the displacement cascade structure and are mainly determined by the setting of the OKMC model parameters. This conclusion is not general however. It must be recalled that when only single-defects are mobile, the differences in cluster frequencies in the long term differ by almost a factor of three when initial cascades had different internal structures (obtained by MD or in the BCA).

6. Conclusion

The effect of using databases of displacement cascades obtained with different potentials, codes and approaches in the radiation damage source term has been studied by object kinetic Monte Carlo. Parameter sets reflecting different assumptions about defect cluster mobility have been employed in order to address the question of which parameters have the greatest influence on defect cluster evolution in the long term. The answer turns out to be complex. The size evolution of vacancy clusters depends on the initial population and spatial distribution of vacancies, but also of interstitials, and vice-versa. The problem is therefore non-linear and its solution depends on the different parameters governing the evolution kinetics in a non-intuitive way.

What is shown in the present work is the existence of an interplay between the parameters controlling the cluster mobility and the structure of the defect sources that are the displacement cascades. In the range investigated, defect mobility parameters are found to affect the order of magnitude of cluster populations. The cascade structure is found to be important in the long term only when the mobility of clusters is inhibited or when it is enhanced above a certain limit. While it clearly appears that the cascade structure may affect the long-term evolution, the structural features that are important for this evolution are not yet identified and this is also an open question which we hope to answer in a next step beyond the present work.

Acknowledgement

Part of this work is achieved in the frame of the European Integrated Project 'PERFECT' (FI6O-CT-2003-508840). Research of R.E. Stoller was supported by the Division of Materials Sciences and Engineering, US Department of Energy under contract DE-AC05-00OR22725 with UT Battelle, LLC.

References

[1] C. Domain, C.S. Becquart, L. Malerba, J. Nucl. Mater. 335 (2004) 121.
[2] M.J. Caturla, N. Soneda, E. Alonso, B.D. Wirth, T. Diaz de la Rubia, J.M. Perlado, J. Nucl. Mater. 276 (2000) 13.
[3] L. Malerba, C.S. Becquart, M. Hou, C. Domain, Philos. Mag. A 85 (2005) 417.
[4] C.S. Becquart, C. Domain, L. Malerba, M. Hou, Nucl. Instrum. and Meth. B. 228 (2005) 181.
[5] M.W. Finnis, 'MOLDY6-A Molecular Dynamics Program for Simulation of Pure Metals,' AERE R-13182, UKAEA Harwell Laboratory, Harwell, UK, 1988.
[6] C.S. Becquart, C. Domain, A. Legris, J.C. Van Duysen, J. Nucl. Mater. 280 (2000) 73.
[7] M.T. Robinson, Phys Rev. B 40 (1989) 10717.
[8] S.M. Ludwig, D. Farkas, D. Pedraza, S. Schmauder, Model. Simul. Mater. Sci. Eng. 6 (1998) 19.
[9] M.W. Finnis, J.E. Sinclair, Phil. Mag. A50 (1984) 45 and Erratum, Phil. Mag. A53 (1986) 161.
[10] A.F. Calder, D.J. Bacon, J. Nucl. Mater. 207 (1993) 25.
[11] R.E. Stoller, J. Nucl. Mater. 276 (2000) 22.
[12] R.E. Stoller, A.F. Calder, J. Nucl. Mater. 283–287 (2000) 746.
[13] L. Malerba, J. Nucl. Mater., in press, doi:10.1016/j.jnucmat.2006.02.023;
D.A. Terentyev, C. Lagerstedt, P. Olsson, K. Nordlund, J. Wallenius, C.S. Becquart, L. Malerba, J. Nucl. Mater., in press, doi:10.1016/j.jnucmat.2006.02.020.
[14] J.F. Ziegler, J.P. Biersack, U. Littmark, in: 'Stopping and Ranges of Ions in Solids', Pergamon, New York, 1985, p. 25.
[15] M. Hou, Z.-Y. Pan, Radiat. Eff. 142 (1997) 483.
[16] M. Hou, Phys. Rev. B 31 (7) (1985) 4178.
[17] W.M. Young, E.W. Elcock, Proc. Phys. Soc. 89 (1966) 735.
[18] Yu.N. Osetsky, D.J. Bacon, A. Serra, B.N. Singh, S.I. Golubov, J. Nucl. Mater. 276 (2000) 65.
[19] F. Willaime, C.C. Fu, M.C. Marinica, J. Dalla Torre, Nucl. Instrum. and Meth. B 228 (2005) 92.
[20] M. Eldrup, B.N. Singh, S.J. Zinkle, T.S. Byun, K. Farrell, J. Nucl. Mater. 307–311 (2002) 912;
M. Eldrup, B.N. Singh, J. Nucl. Mater. 323 (2003) 346.
[21] A. Souidi, M. Hou, C.S. Becquart, C. Domain, J. Nucl. Mater. 295 (2001) 179.
[22] R.E. Stoller, MRS Symp. Proc. 650 (2001) R3.5.1.
[23] Yu. N. Osetsky, D.J. Bacon, Nucl. Instrum. and Meth. B 202 (2003) 31.